

Fast Breaker Failure Backup Protection for HVDC Grids

Willem Leterme, Sahar Pirooz Azad and Dirk Van Hertem

Abstract—This paper proposes a fast breaker failure backup protection algorithm for HVDC grids. The main requirement for HVDC grid protection is the operation speed due to fast rising dc fault currents. Beside a fast primary protection system, fast backup protection must be provided in case of primary protection system failure. Conventional ac backup protection uses extensive time delays that ensure operation of the backup protection system only after failure of the primary protection system. The breaker failure backup protection proposed in this paper minimizes the fault clearing time by initiating backup protection actions and discrimination between cleared and uncleared faults before full fault clearance by the primary protection system. Reliable discrimination is achieved by using both voltage and current measurements. The proposed backup protection algorithm is applied to an HVDC grid test system and simulation results show that the backup protection system can reliably clear faults in case of primary protection system failure.

Index Terms—backup protection, HVDC grid, power system protection, power system transient, VSC HVDC

I. INTRODUCTION

HVDC grids based on voltage source converter (VSC) technology are considered to be part of the future electricity system [1]. These grids can be used to reliably transfer bulk power over large distances, e.g. from an offshore wind farm to the mainland ac grid [2]. An essential part of a reliable grid is the protection system. For future HVDC grids, the protection system design is seen as a main technical challenge as the time scale for HVDC grid protection is ten to hundred times smaller than for ac grid protection [3].

A dc fault current in an HVDC grid has a high rate of rise and reaches a high steady-state value [4]. This puts stringent constraints on the HVDC grid protection system, as fault currents must be interrupted quickly to avoid damage to the grid's components. In the literature, various relaying algorithms have been proposed for fast and selective HVDC grid primary protection [5]–[8]. The aim of the selective primary protection methods is to contain the fault as much as possible to the faulted line, by interrupting the fault current with fast breakers only at the faulted line [9]. By contrast, non-selective fault clearing strategies interrupt dc fault currents

by combined action of multiple elements in the HVDC grid such as converters with fault blocking or fault current limiting capability [10]–[14]. In this approach, the dc fault typically affects a larger part of the grid or even the full HVDC grid. As non-selective methods are typically proposed for smaller systems, only selective fault clearing strategies are considered in this paper.

For selective protection, a backup protection system is needed in case of primary protection system failure [15]. Failures in the primary protection system can be caused by primary relay, breaker or communication system malfunctioning [16]. In ac systems, conventional breaker failure backup protection systems only operate with a certain delay after failure of the primary protection system in clearing the fault. This provides the primary protection system enough time to initially deal with the fault [15].

A backup protection system for HVDC grids has been proposed in [5]. If the current through the primary breaker is not zero after the time for the primary protection system to fully clear the fault, the adjacent breakers are tripped. The disadvantage of this method, which is similar to conventional ac backup protection systems, is its long fault clearance time which results in stringent breaker requirements [17]. In [18], the dc breaker failure backup protection algorithm is based on the breaker internal measurements to determine if the breaker has operated successfully. Fast backup protection is achieved by identifying breaker failure during the attempt of the primary protection system to clear the fault. Although this backup protection algorithm can be very fast, its dependence on the breaker's internal design limits its use in multi-vendor systems.

This paper proposes a fast breaker failure backup protection algorithm for HVDC grids. The proposed backup protection algorithm discriminates cleared faults from uncleared ones during the fault clearing process of the primary protection system. Since the proposed backup protection system only uses primary voltage and current measurements at the line ends, its performance is independent of breaker characteristics.

The paper is structured as follows: Section II gives an introduction to HVDC grid primary and backup protection systems. In Section III, the HVDC grid and its component's models are presented. Besides, this section provides an analysis of the waveforms occurring after a fault in the test system. Section IV presents the breaker failure backup protection algorithm. The results of the application of the backup protection algorithm to the HVDC grid are presented Section V. Finally, conclusions are given in Section VI.

The work of W. Leterme is supported by a research grant from the Research Foundation-Flanders (FWO).

The research leading to these results has received funding from the People Programme (Marie Curie Actions) of the European Union's Seventh Framework Programme (FP7/2007-2013) under REA grant agreement 317221.

W. Leterme, S. Pirooz Azad, and D. Van Hertem are with the EnergyVille/Electa research group, KU Leuven, Heverlee, Belgium (willem.leterme@esat.kuleuven.be, sahar.piroozazad@esat.kuleuven.be, dirk.vanhertem@esat.kuleuven.be)

Paper submitted to the International Conference on Power Systems Transients (IPST2015) in Cavtat, Croatia June 15-18, 2015

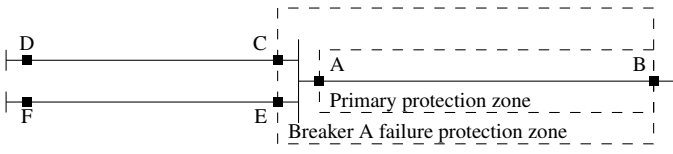


Fig. 1. Protection zones and local backup protection.

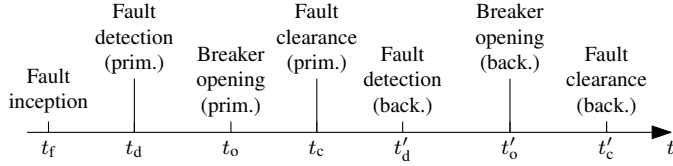


Fig. 2. Time course of fault clearance by primary and breaker failure backup protection.

II. HVDC GRID PROTECTION

To provide selective tripping of breakers, the power system is typically split into several protection zones (Fig. 1) [19]. Each protection zone has a primary protection system that clears faults within its zone as fast as possible, e.g. line AB for relays located at A and B. If any of the breakers associated to the primary protection zone fail to clear the fault, backup protection must be provided to limit the fault impact to the grid [16]. In the system of Fig. 1, breakers located at C and E must be tripped to interrupt the fault current in case of failure of the breaker at location A.

A time course of fault clearance by primary and breaker failure backup protection systems is shown in Fig. 2. A fault is detected by the primary protection system at a certain time t_d after fault inception at time t_f . If the primary breaker operates properly, the breaker opens at t_o and the fault is fully cleared by the primary protection system at t_c . In case of breaker failure, the backup protection system detects the uncleared fault at t'_d , opens the adjacent breakers at t'_o and clears the fault at t'_c .

In HVDC grids, two main requirements are imposed to the protection system; reliability and speed of operation. First, reliable protection implies a secure backup protection, i.e. the backup protection system must not act in case no action is required [15]. As fault clearance by backup protection leads to disconnection of a larger part of the grid (Fig. 1), the backup protection must not operate before the primary protection. Second, fast fault current interruption is required to reduce requirements on the grid components and breakers or to avoid collapse of the dc voltage. To enhance the reliability of the protection system, a large time delay on backup protection operation is desirable, as it allows the primary protection system to act first. However, the requirement of a fast primary and backup protection system impedes the use of large time delays.

III. HVDC GRID MODEL AND DC FAULT ANALYSIS

A. HVDC grid model

Fig. 3 shows the four-terminal HVDC grid test system used in the studies of this paper [20]. In this test system, four converters are connected via five cables to form a meshed

TABLE I
CABLE PARAMETERS AT 1 MHz.

Surge impedance Z_c	33.7 Ω
Traveling wave speed v_c	183.46 km/ms

HVDC grid. A dc breaker is included at the end of each cable. A reactor that limits the current rate of rise is located in series with each dc breaker. The system parameters and components models are taken from [20], except that the series inductor value has been lowered to 50 mH. This section briefly discusses the models of the cables, converters and breakers for transient simulation. The simulations have been performed in PSCAD.

1) *Cable model*: To accurately simulate the high frequency transient behavior after a dc fault, the cables are represented by the frequency dependent (phase) cable model available in PSCAD. This is a distributed parameter model which incorporates the frequency dependency of the cable parameters [21]. The cable's surge impedance and traveling wave speed (at a high frequency) are given in Table I.

2) *Converter model*: Half-bridge modular multilevel converters are considered in this study and are modeled by the continuous converter model with blocking capability [22]. This model represents every arm as a continuous voltage source rather than modeling all individual submodules. This approach speeds up the simulation while providing adequate accuracy.

An important part of the converter model is the converter internal protection. As the insulated gate bipolar transistors (IGBT) must be protected against overcurrents, they are blocked in case of faults. The maximum instantaneous overcurrent that an IGBT can safely turn off is around 2 times the IGBT continuous current. In this study, the converter IGBTs are blocked whenever the current exceeds 1.6 times the continuous current.

3) *Breaker model*: Dc breakers as shown in Fig. 4 are considered for this study [20]. In normal operation, the breaker forms a closed circuit. In case of a fault, the breaker inserts a countervoltage after a certain time delay (t_{br}). This countervoltage is determined by the rating of the parallel surge arrester and is typically 1.5 times the rated dc voltage (480 kV in this case). The time delay t_{br} represents the time required by the dc breaker to open and is assumed to be 2 ms for hybrid dc breakers [9].

B. Fault analysis

Fig. 5 shows the voltage and current for a fault in the middle of link 13 of the test system of Fig. 3. The fault occurs at t equal to 0 ms and creates a traveling wave that arrives at the terminals of link 13 at t equal to 0.54 ms due to a finite traveling wave speed. The traveling waves that are reflected against the inductor, as seen in the voltage waveform, can be used by the primary protection system to swiftly detect the fault and identify the faulted line [7], [8], [23].

If the primary protection fails to clear the fault (solid line), the current increases to a high steady-state value and the voltage diminishes to a near-zero value. If the breaker acts

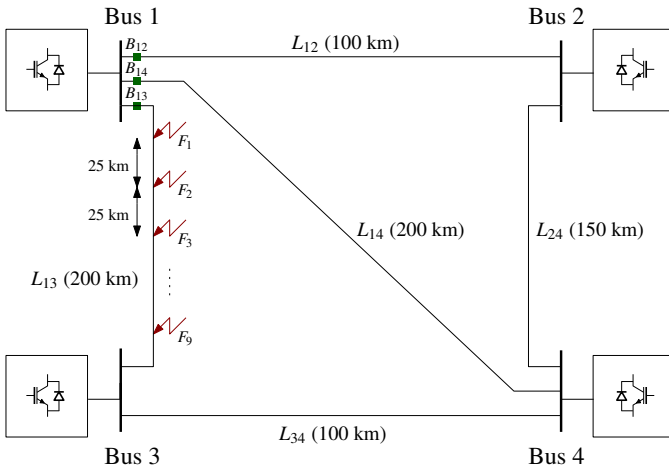


Fig. 3. Four-terminal HVDC grid test system

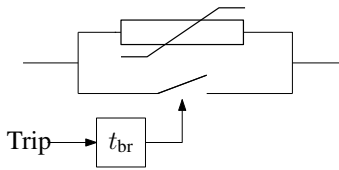


Fig. 4. Hybrid HVDC breaker model.

properly, the current continues to increase until the breaker opening instant (t_0). As the breaker opens, the voltage rises above the nominal value due to the insertion of the surge arrester in series with the line. This drives the current to zero, whereas the voltage reaches its steady-state prefault value.

IV. PROPOSED BREAKER FAILURE BACKUP PROTECTION ALGORITHM

A. Overview

Fig. 6 shows the schematic of the proposed breaker failure backup protection system. For the primary protection of line AB at relay A, voltage and current measurements are used. Upon detection of a fault on line AB, the primary relay R_{prim}^A sends a trip signal to breaker located at A and starts a timer which imposes a delay t_{pb} on the operation of the breaker failure backup relay R_{bf}^A . To prevent the backup breakers to open before the primary breakers, a minimal delay equal to the breaker operation time t_{br} is required. After the delay, the relay R_{bf}^A uses the current and voltage measurements to distinguish a fault that is cleared from one which remains uncleared. If the fault remains uncleared, the breakers located at C and E trip to block the fault current infeed from the rest of the system.

B. Principle

The principle of the proposed breaker failure backup protection algorithm can be explained by plotting the loci of the instantaneous voltage and current in the voltage-current plane (UI-plane). As an example, the loci of the voltage and current for the fault in the middle of link 13 have been plotted in Fig. 7, for the case in which the fault has been cleared by the primary protection system and the case in which the

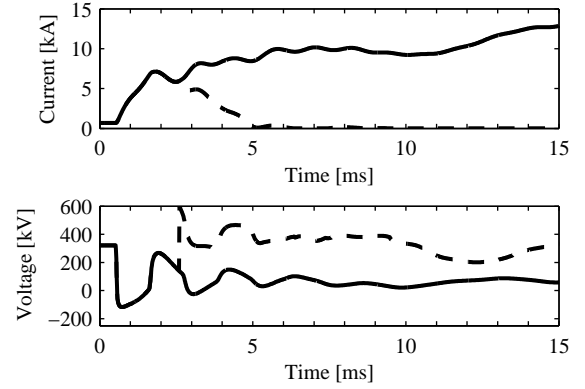


Fig. 5. Voltage and current at R_{13} for a fault in the middle of link 13 (solid: uncleared, dashed: cleared by primary protection).

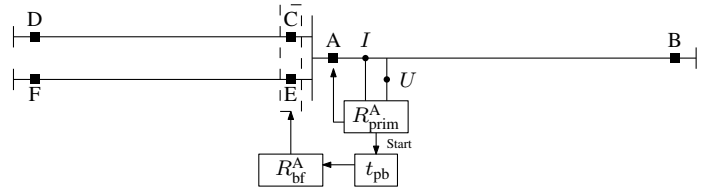


Fig. 6. Overview of proposed backup protection system.

fault remains uncleared. The waveforms for both cases start at the nominal dc voltage and the pre-fault current, which are respectively 320 kV and 0.7 kA. After a fault occurs, the voltage drops and the current increases. Before the breaker opening instant t_0 , the loci of the voltage-current samples coincide for both the uncleared and cleared fault. For an uncleared fault after t_0 , the voltage decreases to a low value whereas the current increases to a high value. For the case in which the fault is cleared by the primary protection system, the voltage again increases and the current decreases to zero after t_0 . The markers in Fig. 7 indicate samples of the cleared and uncleared fault that are taken with time intervals of 0.2 ms after the breaker opening instant t_0 . The proposed breaker failure backup protection algorithm uses the distinction between these samples to discriminate cleared faults from uncleared faults, already during the attempt of the primary protection system to clear the fault.

Fig. 8 illustrates the relay characteristic of the proposed backup protection algorithm, together with a sketch of the loci of voltage and current for a fault that is cleared by the primary protection system and an uncleared one. The arrows indicate the change of the voltage-current loci in function of time. The pre-fault voltage and current are indicated by U_0 and I_0 . At the breaker opening instant t_0 , the voltage and current are denoted by (U_c, I_c) . The steady-state post-fault values for the cleared and uncleared faults are respectively indicated by $(U_c, 0)$ and (U_{uc}, I_{uc}) .

The proposed backup protection algorithm divides the UI-plane into two regions, i.e. cleared fault and uncleared fault. The border of the region consists of 3 segments, which are an overcurrent threshold at high voltages (1), an overcurrent threshold at low voltages (3) and a sloped threshold (2), further

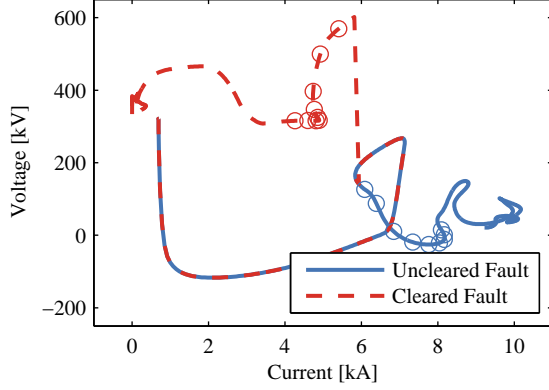


Fig. 7. Locus of voltage and current in UI-plane for cleared and uncleared fault in middle of line 13.

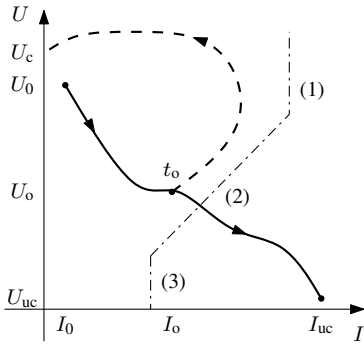


Fig. 8. Principle of the proposed local backup protection algorithm (solid line: uncleared fault, dashed line: cleared fault, dash-dotted line: backup relay characteristic).

referred to as UI-threshold. By determining the region to which the locus of the instantaneous voltage and current belongs, cleared faults can be discriminated from uncleared ones. The distinction between cleared and uncleared faults can be made only after the breaker opening instant t_o . The remainder of this section focuses on determination of this latter threshold.

C. Determination of UI-threshold

Linear discriminant analysis (LDA) is used to find the UI-threshold [24]. LDA is a method that projects sets of samples into a direction that maximizes the separability among them. This direction is perpendicular to the slope of the UI-threshold. The projection of each sample (containing several features) results in a transformed sample with a lower feature dimension. Breaker failure backup protection is thus achieved by comparing the transformed voltage-current samples to a scalar threshold.

The fault samples, denoted by x , consist of two features $(i(t), u(t))$ and are obtained via simulation of a number of faults along the line where the breaker for which the backup protection system is designed, is located. The samples are obtained within the time interval $[t_o, t_{d'}]$ and are sampled with frequency $1/\Delta t$. Let X_1 and X_2 be the sets of voltage and

current samples for uncleared and cleared faults, then:

$$X_1 = \{(i_{uc}(\Delta t), u_{uc}(\Delta t)), (i_{uc}(2\Delta t), u_{uc}(2\Delta t)), \dots, (i_{uc}(n\Delta t), u_{uc}(n\Delta t))\} \quad (1)$$

$$X_2 = \{(i_c(\Delta t), u_c(\Delta t)), (i_c(2\Delta t), u_c(2\Delta t)), \dots, (i_c(n\Delta t), u_c(n\Delta t))\}, \quad (2)$$

For both sets, a matrix S_i can be defined as:

$$S_i = \sum_{x \in X_i} (x - \bar{x}_i)(x - \bar{x}_i)^T, \quad (3)$$

with \bar{x}_i the mean of the set X_i . The sum of matrices S_1 and S_2 is denoted by S_w . The slope w^M of the direction that maximizes separability between samples of both sets can then be found by:

$$w^M = \max_w S_w^{-1}(\bar{x}_1 - \bar{x}_2). \quad (4)$$

Projection of samples from X_1 and X_2 onto this line yields two new (one-dimensional) sets Y_1 and Y_2 , where y_i can be obtained by:

$$y_i = (w^M)^T x_i. \quad (5)$$

Cleared and uncleared faults are distinguished by comparing these transformed samples against a threshold y_{thr} . This threshold is obtained by:

$$y_{thr} = \frac{y_1^d + y_2^d}{2}, \quad (6)$$

where y_1^d and y_2^d are the closest transformed samples from X_1 and X_2 sets, respectively.

The direction w^M is perpendicular to the slope of the UI-threshold, $w^{M,2}$, which can thus be found by:

$$w^{M,2}(w^M)^T = I. \quad (7)$$

The threshold (2) crosses the point (u_{thr}, i_{thr}) that corresponds to threshold y_{thr} :

$$\begin{bmatrix} u_{thr} \\ i_{thr} \end{bmatrix} = ((w^M)^T)^{-1} y_{thr}. \quad (8)$$

V. RESULTS

This section discusses the results obtained from applying the proposed backup protection algorithm to the test system of Fig. 3. As an example, the results associated with B_{13} failure backup protection are presented.

A. Determination of the UI-threshold

Fig. 9 shows the samples obtained from applying 9 faults at equally-spaced distances on line 13 of the test system of Fig. 3. The time between each consecutive sample is 0.2 ms. Based on a current threshold, the minimal amount of time necessary to distinguish between cleared and uncleared faults is 0.4 ms. Alternatively, cleared and uncleared faults can be immediately distinguished at t_o using a voltage threshold. However, to fulfil the reliability requirement of the protection system, backup protection actions need to be delayed until a certain time after t_o . At later times, it is not possible to use only a voltage

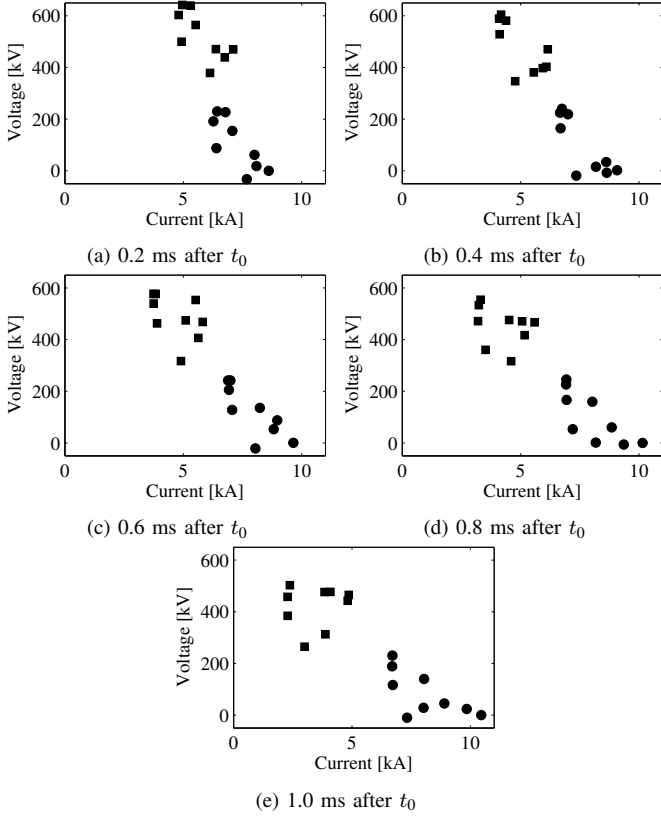


Fig. 9. Locus of voltage and current for faults 1 to 9 (squared markers: cleared fault, dotted markers: uncleared faults).

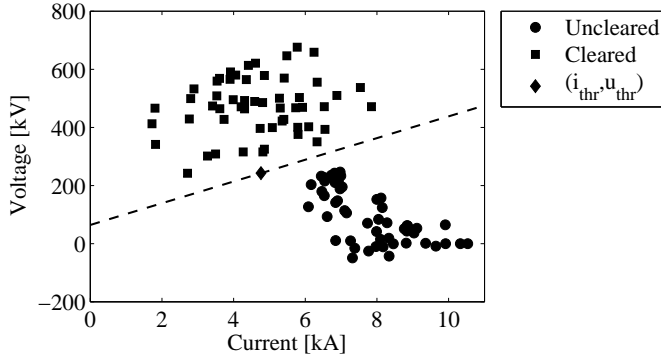


Fig. 10. Threshold determination for B_{13} breaker failure backup protection.

threshold to discriminate cleared and uncleared faults. Therefore, the proposed breaker failure backup protection algorithm makes use of the UI-threshold described in Section IV-B.

Fig. 10 shows the UI-threshold of the backup relay characteristic for all samples of Fig. 9. The slope of the line is 37.36 (kV/kA) and the point (u_{thr}, i_{thr}) is (4.76, 242.4). The scalar threshold y_{thr} is -1.2.

B. Example case in PSCAD

The proposed breaker failure backup protection algorithm has been implemented in PSCAD. To evaluate its performance, a fault is applied in the middle of link 13 and breaker B_{13} is set to fail. The uncleared fault must thus be detected by the backup

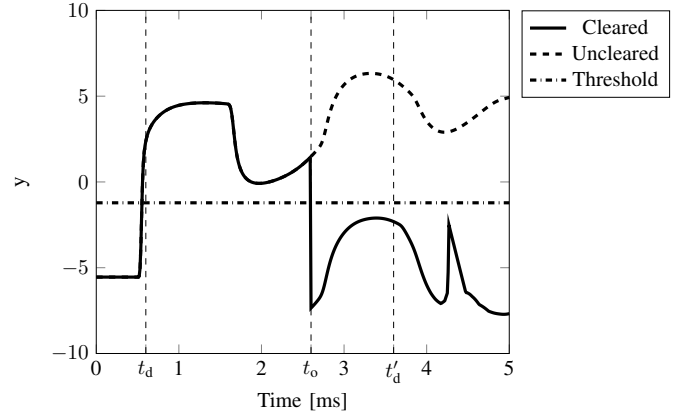


Fig. 11. Transformed samples y for the B_{13} breaker failure backup protection algorithm.

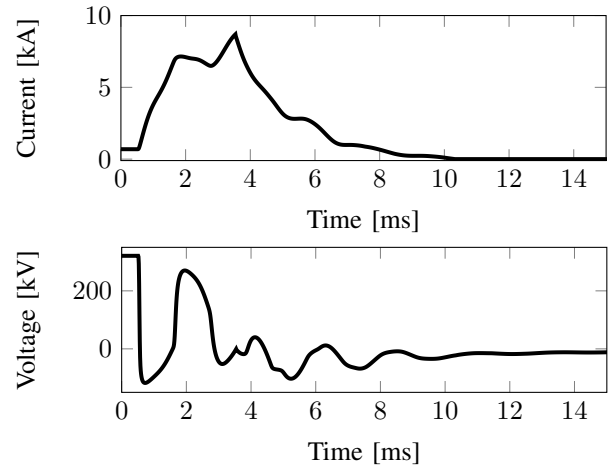


Fig. 12. Voltage and current at R_{13} for a fault in the middle of link 13, cleared by breaker failure backup protection.

protection algorithm using the voltage and current measured at R_{13} . Finally, a tripping signal must be sent to breakers B_{12} , B_{14} and B_{1c} (breaker at the converter terminal). The breaker operation time, t_{br} is 2 ms and the delay on backup protection operation, t_{pb} , is set to 3 ms. The sampling frequency used in the simulation is 100 kHz.

Fig. 11 shows the transformed samples obtained at R_{13} for a cleared and uncleared fault in the middle of link 13 and also the threshold y_{thr} . When the fault reaches the relay, the transformed voltage and current exceeds the threshold y_{thr} . Shortly thereafter, at time t_d , the primary relay detects and identifies a fault on link 13. In case of fault clearance by the primary breaker, the transformed voltage and current returns to a value below the threshold value y_{thr} . If the primary breaker fails to interrupt the fault current, the transformed voltage and current remain above the threshold y_{thr} . In this case, the breaker failure backup protection algorithm indicates an uncleared fault at t'_d and trips all breakers at bus 1. In the example study case, t'_d is 3.65 ms, which is 3 ms after fault detection by the primary relay. The time delay for backup protection system operation, t_{pb} , can be adjusted based on the required speed and reliability of the HVDC grid protection

system.

Fig. 12 shows the voltage and current at R_{13} for a fault in the middle of link 13 that is cleared by the backup protection system. The fault clearance by the backup protection system starts at 3.65 ms (t'_d), and the fault is fully cleared 10 ms after the fault inception instant. The backup protection system acts faster compared to the conventional approach applied to ac systems, as in the latter case the minimal delay for the backup protection is determined by full fault clearance by the primary protection system. The minimal delay for the fault in the middle of link 13 is 5 ms after fault inception (Fig. 5).

In conclusion, the proposed breaker failure backup protection speeds up the operation of the backup protection system by lowering the breaker failure detection time compared to application of the conventional approach as used in ac systems. As a consequence, the system is subject to low voltages and high currents for a smaller amount of time compared to the conventional approach, which results in lower requirements on components and less impact of the disturbance on the system.

VI. CONCLUSION

The proposed breaker failure backup protection algorithm achieves a high speed of operation by discriminating faults which are cleared by the primary protection system from uncleared ones already during the attempt of the primary protection system to clear the fault. Consequently, the proposed backup protection algorithm is faster than conventional breaker failure backup protection algorithms, which delay breaker failure detection until full fault clearance by the primary protection system. Due to an increased speed of the backup protection system, the HVDC grid is subjected to low voltages and high currents for a smaller amount of time, which leads to lower requirements on components and less impact of fault disturbances on the system.

The algorithm uses the primary voltage and current measurements, which are at each sampling instant transformed to a scalar value using linear discriminant analysis. The cleared faults are distinguished from the uncleared ones by comparing the scalar value to a threshold. To demonstrate its effectiveness, the breaker failure backup protection algorithm has been applied to an HVDC grid test system implemented in PSCAD. The threshold for the breaker failure backup protection algorithm has been found by simulation of various faults along the line in the test system for which the backup protection is designed. The simulation results show that this threshold can be used to swiftly discriminate faults that are cleared by the primary protection system from uncleared ones.

REFERENCES

- [1] ENTSO-E. (2012, Jul.) Ten-year network development plan 2012. [Online]. Available: <https://www.entsoe.eu/publications/major-publications/Pages/default.aspx>

- [2] J. De Decker and P. Kreutzkamp, "Offshore Electricity Grid Infrastructure in Europe, Final Report," OffshoreGrid, Tech. Rep., 2011.
- [3] D. Van Hertem and M. Ghandhari, "Multi-terminal VSC HVDC for the European supergrid: Obstacles," *Renewable and Sustainable Energy Reviews*, vol. 14, no. 9, pp. 3156 – 3163, 2010.
- [4] D. Van Hertem, M. Ghandhari, J. Curis, O. Despouys, and A. Marzin, "Protection requirements for a multi-terminal meshed DC grid," in *CIGRE 2011 Bologna Symp.*, Bologna, Italy, 13-15 Sep. 2011, 8 p.
- [5] J. Descloux, "Protection contre les courts-circuits des réseaux à courant continu de forte puissance," Ph.D. dissertation, Université de Grenoble, Grenoble, France, Sep. 2013.
- [6] K. De Kerf, K. Srivastava, M. Reza, D. Bekaert, S. Cole, D. Van Hertem, and R. Belmans, "Wavelet-based protection strategy for dc faults in multi-terminal VSC HVDC systems," *IET Generation, Transmission & Distribution*, vol. 5, no. 4, pp. 496–503, April 2011.
- [7] J. Sneath and A. Rajapakse, "Fault detection and interruption in an earthed hvdc grid using rocov and hybrid dc breakers," *IEEE Trans. Power Del.*, vol. PP, no. 99, pp. 1–1, 2014.
- [8] W. Leterme, J. Beerten, and D. Van Hertem, "Non-unit protection for hvdc grids with inductive cable termination," *IEEE Trans. Power Del.*, 2014, [submitted for publication].
- [9] J. Häfner and B. Jacobson, "Proactive Hybrid HVDC Breakers: A key innovation for reliable HVDC grids," in *CIGRE Bologna Symp.*, Bologna, Italy, 13- 15 Sep. 2011, 8 pages.
- [10] C. Barker, R. Whitehouse, A. Adamczyk, and M. Boden, "Designing fault tolerant hvdc networks with a limited need for hvdc circuit breaker operation," in *Proc. CIGRE 2014*, Paris, France, 24-29 Aug. 2014, 11 pages.
- [11] C. Barker and R. Whitehouse, "An alternative approach to HVDC grid protection," in *Proc. IET ACDC 2012*, Birmingham, UK, 4-6 Dec. 2012, 6 pages.
- [12] M. Hajian, L. Zhang, and D. Jovcic, "Dc transmission grid with low speed protection using mechanical dc circuit breakers," *IEEE Trans. Power Del.*, vol. PP, no. 99, pp. 1–1, 2014.
- [13] D. Schmitt, Y. Wang, T. Weyh, and R. Marquardt, "DC-side fault current management in extended multiterminal-HVDC-grids," in *Proc. IEEE SSD 2012*, Chemnitz, Germany, Mar. 2012, 5 pages.
- [14] M. Merlin, T. Green, P. Mitcheson, D. Trainer, R. Critchley, W. Crookes, and F. Hassan, "The Alternate Arm Converter: A new hybrid multilevel converter with dc-fault blocking capability," *IEEE Trans. Power Del.*, vol. 29, no. 1, pp. 310–317, Feb 2014.
- [15] P. Anderson, *Power System Protection*. Hoboken, NJ, USA: J. Wiley & Sons, 1998.
- [16] W. A. Elmore, *Protective Relaying, Theory and Applications*. New York, NY: Marcel Dekker, Inc., 2004.
- [17] CIGRÉ WG B4-52, "HVDC Grid Feasibility Study," CIGRÉ, Tech. Rep., 2013.
- [18] L. Juhlin, "Fast breaker failure detection for hvdc circuit breakers," Patent WO 2012/136244 A1, Oct. 2012.
- [19] S. Horowitz and A. Phadke, *Power System Relaying*. Hoboken, NJ, USA: J. Wiley & Sons, 2008.
- [20] W. Leterme, N. Ahmed, L. Ångquist, J. Beerten, D. Van Hertem, and S. Norrga, "A new HVDC grid test system for HVDC grid dynamics and protection studies in EMTP," in *Proc. IET ACDC*, Birmingham, UK, 10-12 Feb. 2015, 7 pages.
- [21] PSCAD. (2010) EMTDC User Guide. [Online]. Available: <https://hvdc.ca/knowledge-library/reference-material>
- [22] N. Ahmed, L. Angquist, S. Norrga, A. Antonopoulos, L. Harnefors, and H.-P. Nee, "A computationally efficient continuous model for the modular multilevel converter," *IEEE Journ. of Emerging And Selected Topics in Pow. Elec.*, vol. 2, no. 4, pp. 1139–1148, Dec 2014.
- [23] J. Descloux, B. Raison, and J.-B. Curis, "Protection algorithm based on differential voltage measurement for mtcd grids," in *Proc. IET DPSP 2014*, 31 Mar.-3 Apr. 2014, 5.
- [24] R. A. Fisher, "The use of multiple measurements in taxonomic problems," *Annals of Eugenics*, vol. 7, no. 2, pp. 179–188, Sep. 1936.